$CH_3O^-$ by 0.5 kcal $mol^{-1}$, a fact which can be entirely explained by electron affinity differences between $CH_3O\cdot$ and $CD_3O\cdot$. The exchange reactions of hydroxide with water, first reported in an earlier publication, were extended by making use of a doubly labeled system. The $D^{18}O^- + H_2O$ reaction was found to proceed with a high overall reaction efficiency to form products which at first sight appear to be dominated by a single proton transfer when compared to a simple statistical model. However, closer examination suggests that only about one-fifth of the initially formed complexes dissociate immediately, while the remainder undergo one or more rotations of a water molecule to form a new complex. The amide–ammonia systems were studied for both combinations of isotopic reactants ($H_2N^- + ND_3$ and $D_2N^- + NH_3$). While significant multiple exchange was observed in both cases, the overall efficiencies are considerably lower than in the hydroxide–water systems. The product distributions can be understood in terms of relative ion–molecule complex lifetimes and dissociation of the complex in competition with scrambling. Finally, the exothermic proton abstraction reaction of amide with $D_2O$ was observed to give 17% $HO^-$ while the more highly exothermic reaction of $DO^-$ with $H_2S$ gives only $HS^-$.

We also demonstrated that hydrogen/deuterium exchange in acid–base systems containing second-row elements is observed to proceed in the gas phase with exchange reagents of the same type, i.e., $DS^-$ undergoes efficient exchange with methanethiol, 2-methyl-2-propanethiol, and hydrogen sulfide. The relative efficiencies of exchange correlate well with the relative acidities and relative ion–dipole binding energies. The lack of exchange reported earlier for $HS^-$ with $CF_3CH_2OD$ is not unexpected when the relative acidities and relative ion–dipole energies are considered. It is expected that $HS^-$ will exchange with a first-row acid closer in acidity to $H_2S$ than $CF_3CH_2OD$, perhaps, for example, $CF_3C(CH_3)_2OD$.

Finally, these systems are ideal candidates for modeling by phase space/RRKM theory. Such studies would provide valuable insight into the detailed pathways involved, including the barriers to rotation discussed above. Further investigations, both in the lab and by theory, will continue to contribute to our understanding of this fundamental process.

**Acknowledgment.** We thank the donors of the Petroleum Research Fund, administered by the American Chemical Society, and the National Science Foundation under Grant CHE-8203110 (to C.H.D. and V.M.B.) for support of this work. We gratefully acknowledge the experimental assistance given by Jonathan Filley and Stephan Barlow.

# Mechanism of Cytochrome *c* Oxidase-Catalyzed Dioxygen Reduction at Low Temperatures. Evidence for Two Intermediates at the Three-Electron Level and Entropic Promotion of the Bond-Breaking Step

**David F. Blair, Stephan N. Witt, and Sunney I. Chan***

*Contribution No. 7140 from the Arthur Amos Noyes Laboratory of Chemical Physics, California Institute of Technology, Pasadena, California 91125.* *Received January 15, 1985*

**Abstract:** The reaction of cytochrome *c* oxidase with dioxygen has been examined by using a modification of the triple-trapping technique (Chance, B.; Saronio, C.; Leigh, J. S., Jr. *J. Biol. Chem.* **1975**, *250*, 9226–9237) in conjunction with EPR spectroscopy. The investigation has been extended to a broader temperature range than previous studies, and several new reaction steps have been resolved. Where possible, the temperature dependences of the rates of individual steps have been measured, enabling estimation of enthalpies of activation. Both the low potential sites ($Fe_a$ and $Cu_A$) and the dioxygen reduction site ($Fe_{a_3}/Cu_B$) have been monitored simultaneously, enabling clarification of the relationship between the electron transfers to the dioxygen reduction site and the events which occur there. The evidence indicates that there are two intermediates at the three-electron level of dioxygen reduction, only the first of which is EPR-detectable. The conversion between these two intermediates, which probably corresponds to the breaking of the dioxygen bond, exhibits a distribution of activation enthalpies which peaks at 18.1 ± 1.6 kcal $mol^{-1}$. Assuming a preexponential factor of $10^{13}$, the corresponding activation entropy is 21.4 ± 8.2 cal $mol^{-1}$ $K^{-1}$, indicating that this process is promoted by entropic factors. Experiments using enzyme reduced by only three electrons confirm the existence of the two different three-electron intermediates proposed. These experiments also indicate that the rate of electron transfer from $Fe_a$ to the $Fe_{a_3}/Cu_B$ site depends upon which intermediate of dioxygen reduction is present at the latter site. Finally, we have obtained evidence that one of the three-electron intermediates of dioxygen reduction, probably a ferryl ion, can react with carbon monoxide at low temperature (211 K) to produce $CO_2$ and a partially reduced enzyme species which exhibits EPR signals characteristic of a magnetically isolated $Cu_B$ center. These results are discussed in terms of the electron-transfer pathways within the enzyme and its mechanisms of dioxygen reduction and energy conservation.

Cytochrome *c* oxidase is the terminal component in the mitochondrial respiratory chain of eukaryotic organisms. In this role, the enzyme catalyzes the rapid reduction of dioxygen to water, using electrons derived from ferrocytochrome *c* (eq 1) and con-

$$4H^+ + O_2 + 4\text{ferrocytochrome } c \rightarrow 2H_2O + 4\text{ferricytochrome } c \quad (1)$$

serves part of the free energy released in this reaction by contributing to the generation of the proton electrochemical potential across the inner mitochondrial membrane.[1] The turnover rate of the enzyme is as high as 400 electrons transferred per second.[2]

Mitochondrial cytochrome *c* oxidase is a large ($M_r$ 170 000) multisubunit protein.[3] The functional monomer contains four metal ions: two coppers, designated $Cu_A$ and $Cu_B$, and two irons

* To whom all correspondence should be addressed.

(1) Wikström, M. *Curr. Top. Membr. Transp.* **1982**, *16*, 303–321.
(2) Vik, S. B.; Capaldi, R. A. *Biochem. Biophys. Res. Commun.* **1980**, *94* (1), 348–354.
(3) Merle, P.; Kadenbach, B. *Eur. J. Biochem.* **1980**, *105*, 499–507.

0002-7863/85/1507-7389$01.50/0 

contained in heme *a* prosthetic groups, designated $Fe_a$ and $Fe_{a_3}$. Two of the metal ions, $Fe_{a_3}$ and $Cu_B$, are situated close (ca. 5 Å) to each other and together constitute the site of dioxygen reduction. The other two metal ions, $Fe_a$ and $Cu_A$, rapidly accept electrons from cytochrome *c* and transfer them to the binuclear site.[4]

The mechanism of dioxygen reduction by the enzyme has been the subject of several investigations.[5-9] It is difficult to study the intermediates formed during the dioxygen reduction reaction under physiological conditions because the reaction is so rapid: the bimolecular rate constant for the combination of dioxygen with the reduced enzyme is $8 \times 10^6$ $M^{-1}$ $s^{-1}$ at room temperature, and most of the ensuing intramolecular electron transfers take place within a millisecond.[9,10] However, the reaction may be slowed by going to lower temperatures (160–200 K). The so-called triple trapping technique, originally developed by B. Chance et al.,[11] has been widely used[7,8] to follow the reaction between dioxygen and cytochrome *c* oxidase at low temperatures. In this method, the enzyme is reduced and then inhibited by the addition of carbon monoxide (CO), which binds tightly to ferrous $Fe_{a_3}$. Oxygen is rapidly stirred into the solution at ca. 250 K, at which temperature the dissociation of CO from the enzyme is sufficiently slow that very little reoxidation of the enzyme occurs. The mixture is then frozen at a temperature at which no reaction will occur (77 K) and is exposed to visible light, which causes the photodissociation of CO from $Fe_{a_3}$. The removal of CO exposes this site for reaction with dioxygen. When the sample is warmed to ca. 160 K, dioxygen binds to $Fe_{a_3}$ and intramolecular electron transfer(s) occur on the time scale of minutes. These reactions can be periodically halted (by rapid cooling of the sample) and the reaction intermediates studied spectroscopically.

Clore and E. Chance[6] used this technique in conjunction with optical spectroscopy to show that at least three distinct intermediates (designated I, II, and III) form in sequence in the low-temperature reaction of dioxygen with cytochrome *c* oxidase. (Intermediates I and III are the same as compounds $A_1$ and B described previously by B. Chance et al.[11]) Intermediate I is probably a species in which dioxygen is bound to ferrous $Fe_{a_3}$ and $Cu_B$ is reduced.[12] Intermediate II is formed from intermediate I when one electron is transferred from one of the other oxidase metal centers ($Fe_a$ or $Cu_A$) to the dioxygen reduction site; intermediate III is produced when the last electron is transferred to this site.

Since this pioneering work, Clore et al.[8] have also followed the intermediates formed during the cytochrome *c* oxidase-catalyzed reduction of dioxygen using combined EPR and optical spectroscopies. EPR permits the determination of the redox states of $Cu_A$ and $Fe_a$ in intermediates I, II, and III. As a result of this more complete study, the sequential reaction scheme required refinement. The EPR experiments showed that the third electron transferred to the dioxygen molecule could originate from either $Fe_a$ or $Cu_A$, so that intermediate II is in fact a mixture of two species. In both of these species, the dioxygen reduction site may be represented formally as $[Fe_{a_3}\text{–O–O–}Cu_B]^{2+}$; the other sites may be represented by $Cu_A^{1+}/Fe_a^{3+}$ in one case or by $Cu_A^{2+}/Fe_a^{2+}$ in the other. These species were designated IIA and IIB, respectively. At 173 K, intermediate IIB is a stable product, while intermediate IIA reaches a peak concentration at 200 s and decays to negligible concentration after 3000 s. Intermediate III is formed from intermediate IIA by the transfer of an electron from $Cu_A$ to the dioxygen reduction site in the molecules in which the initial electron transfer took place from $Fe_a$.

Because both intermediates IIA and IIB contain an odd number of electrons at the dioxygen reduction site, an EPR signal might be expected from these intermediates. Although no EPR signal was reported from this site in the original work of Clore et al., Karlsson et al.[13] subsequently reported a new $Cu_B$ EPR signal associated with the three-electron level of dioxygen reduction (intermediates IIA and IIB). (In referring to the level of dioxygen reduction, we count the electrons donated from the $Fe_{a_3}/Cu_B$ site, so that the transfer of a single electron from one of the other sites generates what we will call a three-electron intermediate of dioxygen reduction.) The signal is unusual in that the portions of the spectrum corresponding to $g_x$ and $g_y$ are not observable, and the portion which is observable at $g_z$ is very resistant to power saturation even at 9 K. This unusual EPR signal was proposed to arise from a $Cu_B$ that is coupled, via dipolar and/or exchange mechanisms, to a nearby, very rapidly relaxing species such as a ferryl $Fe_{a_3}$, which would be expected to have a total spin angular momentum of 1.[14-16]

The observation of a $Cu_B$ EPR signal from the dioxygen reduction site of a three electron-reduced intermediate is significant because it enables the direct observation of subsequent processes occurring at the dioxygen reduction site, and the elucidation of the relationship of these events to the electron transfers from the other sites. In the present work, we have sought to clarify the nature of the three-electron intermediate (or intermediates) and to obtain additional insights into the mechanism of dioxygen reduction by simultaneously examining the kinetics of the electron transfers from the $Cu_A$ and $Fe_a$ sites and the behavior of the unusual $Cu_B$ signal, over a range of temperatures. Several additional reaction steps have been resolved by incubating samples at temperatures higher than those previously used. The results indicate that there are at least two different dioxygen reduction intermediates at the three-electron level. The temperature-dependence data indicate that the conversion between these two intermediates, which we propose involves the breaking of the dioxygen bond, has a large enthalpy of activation but is promoted by entropic factors.

We have confirmed the existence of two different three-electron intermediates of dioxygen reduction by conducting some experiments on partially (ca. three electron) reduced cytochrome *c* oxidase. These experiments have also proven useful in understanding the branched reaction mechanism developed by Clore et al.[8] and described above. Specifically, the results indicate that the rate of electron transfer from $Fe_a$ to the dioxygen reduction site depends significantly upon which dioxygen-reduction intermediate is present at the latter site: If the electron transferred from $Fe_a$ to the $Fe_{a_3}/Cu_B$ site is the third electron to take part in dioxygen reduction, the transfer takes place rapidly, but if it is the fourth electron, the transfer is quite slow.

In the course of examining the temperature dependences of the various steps in the dioxygen reduction reaction, we have discovered that a second, readily saturable $Cu_B$ EPR signal, identical with that reported by Karlsson and Andréasson[17] using a different means of preparation, is produced in good yield at relatively low (211 K) temperature. A signal assignable to low-spin $Fe_{a_3}$ adjacent to reduced $Cu_B$ also appears at 211 K and higher temperatures. A variety of evidence suggests that the production of these signals involves the reaction of a three-electron intermediate of dioxygen reduction, probably a ferryl ion, with carbon monoxide to generate $CO_2$ and an enzyme species which is reduced by one electron at the $Fe_{a_3}/Cu_B$ site.

(4) Wikström, M.; Krab, K.; Saraste, M. "Cytochrome Oxidase—A Synthesis"; Academic Press: New York, 1981.
(5) Chance, B.; Leigh, J. S., Jr. *Proc. Natl. Acad. Sci. USA.* **1977**, *74*, 4777–4780.
(6) Clore, G. M.; Chance, E. M. *Biochem. J.* **1978**, *173*, 811–820.
(7) Clore, G. M.; Chance, E. M. *Biochem. J.* **1978**, *175*, 709–725.
(8) Clore, G. M.; Andréasson, L. E.; Karlsson, B.; Aasa, R.; Malmström, B. G. *Biochem. J.* **1980**, *185*, 139–154.
(9) Gibson, Q. H.; Greenwood, C. *Biochem. J.* **1963**, *86*, 541–554.
(10) Greenwood, C.; Gibson, Q. H. *J. Biol. Chem.* **1967**, *242* (8), 1782–1787.
(11) Chance, B.; Saronio, C.; Leigh, J. S., Jr. *J. Biol. Chem.* **1975**, *250*, 9226–9237.
(12) Babcock, G. T.; Jean, J. M.; Johnston, L. N.; Palmer, G.; Woodruff, W. H. *J. Am. Chem. Soc.* **1984**, *106*, 8305–8306.
(13) Karlsson, B.; Aasa, R.; Vänngård, T.; Malmström, B. G. *FEBS Lett.* **1981**, *131*, 186–188.
(14) Hansson, O.; Karlsson, B.; Aasa, R.; Vänngård, T.; Malmström, B. G. *EMBO J.* **1982**, *1* (11), 1295–1297.
(15) Theorell, H.; Ehrenberg, A. *Arch. Biochem. Biophys.* **1952**, *41*, 442–461.
(16) Schulz, C.; Chiang, R.; Debrunner, P. G. *J. Phys.* **1979**, *40*, C2-534–536.
(17) Karlsson, B.; Andréasson, L. E. *Biochim. Biophys. Acta* **1981**, *635*, 73–80.

## Experimental Section

**Sample Preparation.** Beef heart cytochrome *c* oxidase was isolated by the method of Hartzell and Beinert.[18] The final pellet was dissolved in 0.5% Tween-20, 50 mM potassium phosphate, pH 7.4, or 50 mM TrisCl, pH 7.4; ammonium sulfate and cholate were removed from the enzyme by dialysis against the same buffers. The enzyme was stored at −80 °C until ready for use. The purified enzyme contained 8 nM heme *a* ((mg protein)$^{-1}$) and its activity was 9.0 nmol of $O_2$ reduced min$^{-1}$ ($\mu$g of protein)$^{-1}$. Heme *a* concentration was determined by the pyridine hemochromagen assay.[19] Protein concentration was determined by a modification of the Lowry procedure which includes 1% sodium dodecyl sulfate to solubilize integral membrane proteins.[20] Stock solutions used to prepare EPR samples were typically 0.2–0.3 mM in cytochrome oxidase.

EPR samples for low-temperature kinetic study were prepared in 5 mm o.d. (3.4 mm i.d.) EPR tubes. They were degassed by four to five cycles of evacuation and flushing with argon which had been scrubbed of oxygen by passage through 0.1 M vanadous ion in 2 N HCl followed by passage through 0.02 M NaOH. A small excess (ca. 1.2 equiv) of NADH (nicotinamide adenine dinucleotide) (Sigma) and 0.01 equiv of phenazine methosulfate were added to the samples under an argon atmosphere, causing complete reduction of the oxidase within 30 min. An equal volume of 80/20 (v/v) ethylene glycol/buffer, which had previously been degassed by four to five cycles of freezing, evacuation, thawing, and stirring, was mixed thoroughly with the reduced enzyme solutions at 4 °C. The argon atmosphere was then exchanged for a 25%/75% mixture of carbon monoxide (CO) (Matheson 99.99%) and scrubbed argon. The samples were cooled to −20 °C and evacuated. One atmosphere of pure oxygen was admitted to the samples in the dark, and they were vigorously agitated for 15–20 s and then frozen in liquid nitrogen. It was found that the use of pure oxygen, rather than air, was important to ensure complete reaction of the oxidase with dioxygen. The frozen solution formed an optically transparent glass. Because CO is bound to the dioxygen reduction site of the cytochrome oxidase, very little (less than 5% in most cases) oxidation of the enzyme occurs during the addition of dioxygen in the dark, as judged by the intensities of the $Fe_a$ and $Cu_A$ EPR signals prior to incubation at temperatures which allow reaction with dioxygen.

In order to remove CO from $Fe_{a_3}$, the samples were photolyzed in a finger Dewar at 77 K by irradiation with a 200-W Hg–Xe arc lamp for 30–40 min with frequent rotation of the sample so that all sides were equally exposed to the light. Following photolysis, samples were stored in liquid nitrogen until ready for use. The reaction with dioxygen was initiated by immersing the sample tubes in *n*-pentane baths kept at the desired temperature by immersion in methanol/ethanol solutions cooled by the addition of liquid nitrogen. It was found to be important to immerse the samples with a stirring action to accelerate thermal equilibration. The reaction was quenched by returning the samples to the liquid nitrogen bath. The *n*-pentane which solidified on the sample tubes was removed prior to examination of the sample by EPR.

For experiments in which the enzyme was initially only partially reduced, enough NADH was added to provide ca. three electrons per oxidase molecule; all other operations were identical with the preparation of the fully reduced enzyme. The extent of reduction was determined from the EPR spectrum obtained after photolysis but prior to incubation at temperatures which allow reaction with dioxygen.

**EPR Spectroscopy.** EPR spectra were recorded on a Varian E-line Century Series X-band spectrometer operating in the absorption mode. The modulation amplitude was 16 G and the modulation frequency 100 kHz. Microwave powers used were 0.02 mW for the $Cu_A$ signal, 0.02 mW or 0.20 mW for the $Fe_a$ signal, and 20 mW for the $Cu_B$ signal.

Sample temperature was controlled with an Air Products Heli-Tran cryostat. The temperature at the sample position was measured before and after spectra were acquired, using a gold-chromel thermocouple in a glycerol-filled EPR tube. The temperature was typically 9 K. Data were rejected if significant (>0.5 K) temperature changes occurred during spectrum acquisition.

For most purposes, EPR intensities were measured as peak heights ($Fe_a$ at $g = 3$) or peak-to-trough distances ($Cu_A$). For purposes of absolute comparisons between signal intensities, the $Cu_A$ signal was double-integrated, using a base line which was determined by the requirement that the first integral be zero, and the $Fe_a$ signal was integrated by the method of Aasa and Vänngård[21] by using the peak at $g = 3$ to estimate the total area. The $Cu_B$ signal was integrated by using the lowest-field hyperfine peak to estimate the total area, using the assumption that the $g_x$ and $g_y$ values are both 1.3, as suggested by lineshape simulations.[14] This integration verified that the observed $Cu_B$ signal intensity corresponded to the number of spins expected on the basis of the kinetic models postulated. For routine relative measurements of the $Cu_B$ signal, the height of the lowest-field hyperfine peak was used; the line width of this peak was observed to remain constant within the uncertainty of the determination.

**Data Analysis.** To determine the temperature dependence of the rate constant for the decay of the $Cu_B$ EPR signal, the decay was investigated over a range of temperatures. The kinetic data for the decay of the $Cu_B$ EPR signal were not well-fitted by a single exponential function. It is thought that nonexponential kinetics for processes in proteins at low temperatures result from the presence of multiple conformations which have different barrier heights for the process.[22-24] At low temperatures, there is insufficient thermal energy to promote interconversions among the various conformations. Thus, all the various activation enthalpies for the process are manifested in the kinetics. Experimentally, a distribution of activation enthalpies is observed, instead of a single, well-defined value.

Austin et al[22] first demonstrated that the nonexponential kinetics for the rebinding of CO to myoglobin at low temperatures could be fitted to the power law given in eq 2. $N(t)$ is the fraction of unbound heme

$$N(t) = C(1 + t/t_0)^{-n} \tag{2}$$

at time $t$. $C$, $t_0$, and $n$ are constants. It should be noted that $n$ and $t_0$ are temperature-dependent constants, so it is more accurate to write $n(T)$ and $t_0(T)$.

Austin et al. showed that the rate of reaction which corresponds to the most probable activation enthalpy, $\Delta H_p^{\ddagger}$, is given by[22]

$$k_p = n/t_0 = \omega \exp[\Delta S^{\ddagger}/R - \Delta H_p^{\ddagger}/RT] \tag{3}$$

where $\omega$ is a frequency prefactor of order $10^{13}$ s$^{-1}$. Thus, by fitting the data from the decay of the $Cu_B$ EPR signal to eq 2, $n(T)$ and $t_0(T)$ may be determined, from which the most probable rate constant in the distribution is obtained. A plot of log $k_p(T)$ vs. $1/T$ then yields the activation entropy and the most probable activation enthalpy.

The $Cu_B$ kinetic data were fitted to the power law by using a nonlinear least-squares computer program which computes the least-squares estimates of $C$, $n$, and $t_0$. Activation enthalpies and entropies were calculated by fitting the ln $k_p$ vs. $1/T$ data, using a linear least-squares program, to the linear form of the Arrhenius relation in eq 3. Error bars on the graphs represent twice the sample standard deviation of the data points from the best fit line in the nonlinear least-squares fit of the kinetic data at each temperature.

The same linear least-squares analysis was also applied to the Arrhenius plot of the kinetic data for $Cu_A$ oxidation. For this process, the rate was estimated by measuring the initial slope to the EPR intensity vs. time curves.

## Results

**Oxidation of $Fe_a$ and $Cu_A$.** Following photolysis of CO from $Fe_{a_3}$ at 77 K, cytochrome *c* oxidase samples were first incubated at temperatures between 166 and 186 K to initiate the intramolecular electron transfers to dioxygen. Optically monitored low-temperature kinetic studies have established that the binding of dioxygen to $Fe_{a_3}$ takes place with a bimolecular rate constant of 81 M$^{-1}$ s$^{-1}$ at 173 K;[8] hence this binding step is not expected to be significantly rate-limiting in our experiments, where the oxygen concentration is ca. 1 mM and the initial electron transfers take place with rates of approimately $2 \times 10^{-3}$ s$^{-1}$ at 173 K. The intermediate which is formed upon dioxygen binding, designated I by Clore et al.,[8] exhibits no EPR signals. Upon incubation at temperatures between 166 and 186 K, electron transfers from $Cu_A$ or $Fe_a$ to the dioxygen reduction site take place, causing the appearance of EPR signals which are characteristic of these metal ions in their oxidized states.

The magnitudes of the $Cu_A$ and $Fe_a$ EPR signals after various times of incubation at 181 K are plotted in Figure 1. The oxidation of $Cu_A$ during the first 30 min at 181 K takes place in at least two phases, as evidenced by the poor quality of a single

(18) Hartzell, C. R.; Beinert, H. *Biochim. Biophys. Acta* **1974**, *368*, 318–338.
(19) "Laboratory Methods in Porphyrin and Metalloporphyrin Research"; Fuhrop, J.-H., Smith, K. M., Eds.; Elsevier: New York, 1975; p 48.
(20) Markwell, M. A. K.; Haas, S. M.; Bieber, L. L.; Tolbert, N. E. *Anal. Biochem.* **1978**, *87*, 206–210.
(21) Aasa, R.; Vänngård, T. *J. Magn. Reson.* **1975**, *19*, 308–315.
(22) Austin, R. H.; Beeson, K.; Eisenstein, L.; Frauenfelder, H.; Gunsalus, I. C.; Marshall, V. P. *Phys. Rev. Lett.* **1974**, *32* (8), 403–405.
(23) Austin, R. H.; Beeson, K. W.; Eisenstein, L.; Frauenfelder, H.; Gunsalus, I. C. *Biochemistry* **1975**, *14* (24), 5355–5373.
(24) Agmon, N.; Hopfield, J. J. *J. Chem. Phys.* **1983**, *79* (4), 2042–2053.

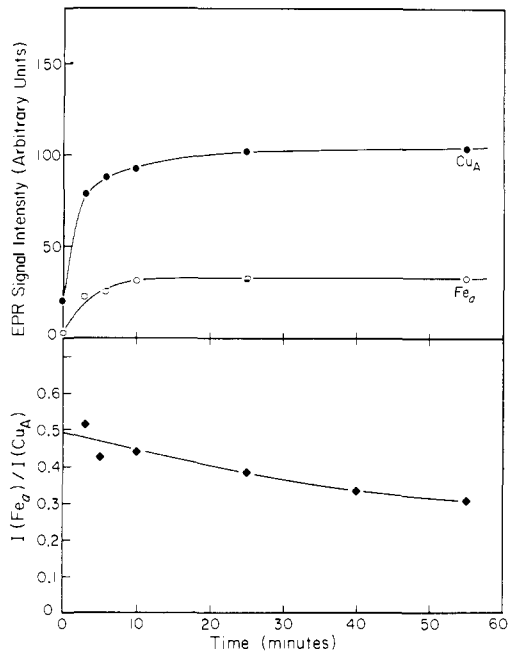


**Figure 1.** Intensities of the EPR signals due to $Cu_A$ and $Fe_a$ during incubation of a reduced cytochrome *c* oxidase sample in the presence of dioxygen at 181 K. Conditions of EPR spectroscopy: temperature 9 K; microwave frequency 9.172 GHz; modulation amplitude 16 G; microwave power 0.02 mW ($Cu_A$) or 0.20 mW ($Fe_a$). Sample preparation, incubation methods, and quantitation of EPR signals are described in the Experimental Section. Bottom: the ratio of the intensities of the $Cu_A$ and $Fe_a$ signals during incubations at the same temperature, showing that the two sites do not follow parallel courses of oxidation.

**Table I** First-Order Rate Constants[a] and Corresponding Temperatures for the Formation of the $Cu_A$ EPR Signal

| temp, K | $k(Cu_A)$, $s^{-1}$ | temp, K | $k(Cu_A)$, $s^{-1}$ |
|---|---|---|---|
| 186.0 | $(1.7 \pm 0.2) \times 10^{-2}$ | 173.0 | $(1.9 \pm 0.1) \times 10^{-3}$ |
| 181.0 | $(4.4 \pm 0.2) \times 10^{-3}$ | 171.0 | $(5.0 \pm 0.2) \times 10^{-4}$ |
| 180.5 | $(4.6 \pm 0.1) \times 10^{-3}$ | 166.0 | $(1.9 \pm 0.2) \times 10^{-4}$ |
| 176.0 | $(1.3 \pm 0.1) \times 10^{-3}$ | | |

[a] First-order rate constants were determined by measuring the initial slopes to the formation curves for the $Cu_A$ signal.

exponential fit to the data. If the analysis is restricted to only the first 3 min of oxidation at 181 K and if data points are taken at shorter intervals, the $Cu_A$ data are satisfactorily fitted by a single exponential (data not shown), indicating that a prior step is not partially rate-limiting. Fits to the $Fe_a$ data are not conclusive with respect to the question of whether the oxidation is monophasic or biphasic owing to the poorer signal-to-noise ratio of this signal. The ratio of the intensities of the $Cu_A$ and $Fe_a$ signals during the initial phase of oxidation is also shown in Figure 1 and demonstrates that the two sites are not oxidized in parallel. After 55 min at 181 K, the intensity of the $Fe_a$ signal corresponded to only ca. 30% of the intensity of the $Cu_A$ signal. In samples which had been thoroughly oxygenated prior to freezing, the intensity of the $Cu_A$ signal corresponded to nearly 100% of the enzyme molecules, as judged by the effect of thawing the samples and remeasuring the $Cu_A$ EPR signal. All these observations agree qualitatively with the results of the combined optical/EPR study of Clore et al.[8] Their results and ours are most satisfactorily accounted for by the reaction sequence shown in Scheme I.

The oxidation of $Cu_A$ was investigated at several temperatures between 166 and 186 K. Because this process is not well-fitted by a single exponential, the rate of the first oxidation step was estimated by measuring the initial slopes of the EPR intensity vs. time curves. The rate constants and corresponding temperatures are presented in Table I. An Arrhenius plot of the data is linear within experimental uncertainty and gives an activation enthalpy and entropy of $13.2 \pm 1.4$ kcal $mol^{-1}$ and $2.8 \pm 7.7$ cal $mol^{-1}$ $K^{-1}$, respectively, assuming a preexponential factor of $10^{13}$ $s^{-1}$.[25] The

**Scheme I**

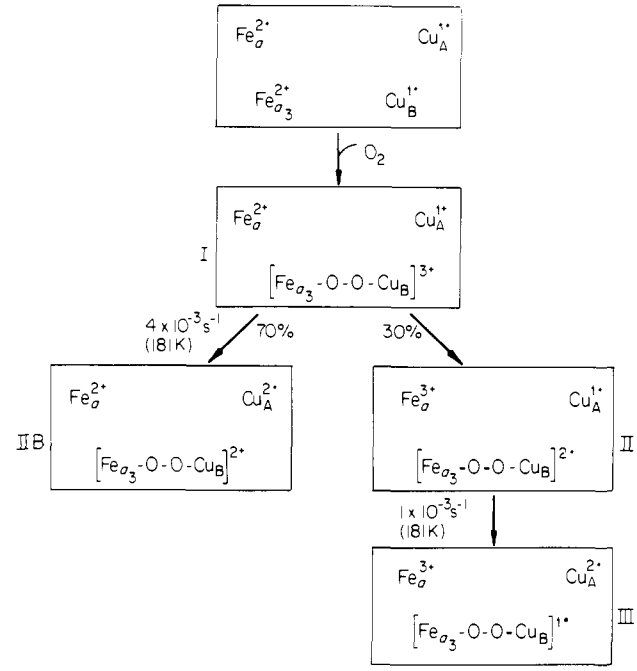


level of $Fe_a$ oxidation which was attained in this early phase of the reaction (and therefore its rate of oxidation) relative to that of $Cu_A$ did not vary significantly over the temperature range examined, indicating that the activation enthalpies for the $Fe_a$ and $Cu_A$ oxidations are similar.

In an infrared absorption study of the photolysis of CO from cytochrome *c* oxidase, Fiamingo et al.[26] have shown that when CO is photolyzed from the enzyme at low (ca. 180 K) temperatures, it first binds to $Cu_B$ and subsequently recombines with $Fe_{a_3}$ in a relatively slow process. While CO remains bound to $Cu_B$, the binding and reaction of dioxygen to form an electron-accepting intermediate is likely to be inhibited. These authors consequently suggested that the dissociation of CO from $Cu_B$ may be rate-limiting in the initial electron-transfer step of the dioxygen reduction reaction as studied by the triple-trapping technique. The rate of recombination of CO with $Fe_{a_3}$ (which parallels its rate of dissociation from $Cu_B$) is $7.4 \times 10^{-3}$ $s^{-1}$ at 181 K; the activation enthalpy for this process is 9.2 kcal $mol^{-1}$.[26] Comparison with our measurements (Table I) shows that the rate of $Cu_A$ oxidation at 181 K is similar (within a factor of 2) at this temperature, whereas the activation enthalpy for $Cu_A$ oxidation is significantly greater.

**Production of the Unusual $Cu_B$ EPR Signal.** The initial transfer of an electron from either $Cu_A$ or $Fe_a$ to the dioxygen reduction site produces an intermediate which contains an odd number of electrons at the dioxygen reduction site. This species gives rise to a copper EPR signal which is distinguished by two unusual properties: It is very difficult to saturate, even at 9 K, and only one of its *g* values is evident in the spectrum.[13,14] This signal has been assigned to $Cu_B$ in close proximity to another paramagnetic ion which undergoes more rapid spin relaxation.[13,14] In Figure 2, the intensity of this signal after various times of incubation at 181 K is shown. The $Cu_B$ EPR spectrum in the $g_z$ region is shown in Figure 3. In agreement with earlier findings,[13] we observe that the early growth of this signal roughly parallels the initial oxidations of $Cu_A$ and $Fe_a$. This result is consistent with the assignment of the signal to an intermediate at the $Fe_{a_3}/Cu_B$ site which is at the three-electron level of dioxygen reduction. The

(25) At 200 K, the Eyring prefactor $kT/h$ is approximately $0.4 \times 10^{13}$ $s^{-1}$; so $1.0 \times 10^{13}$ is likely to be an overestimate. Also, the transmission coefficient $\kappa$ has been taken to be 1.0, the maximum possible. The effect of these assumptions, which probably overestimate the effective frequency prefactor, will be to underestimate the activation entropy.

(26) Fiamingo, F. G.; Altschuld, R. A.; Moh, P. P.; Alben, J. O. *J. Biol. Chem.* **1982**, *257*, 1639–1650.

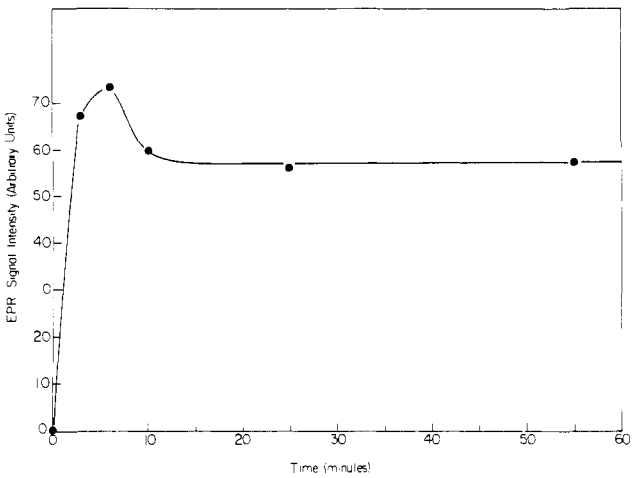


**Figure 2.** Intensity of the unusual $Cu_B$ EPR signal during incubation of a reduced cytochrome *c* oxidase sample in the presence of dioxygen at 181 K. Conditions of EPR spectroscopy were as noted in Figure 1, except the microwave power was 20 mW. Sample preparation, incubation methods, and EPR signal quantitation are described in the Experimental Section. Assuming *g*(perpendicular) values of 1.3 for the $Cu_B$ signal,[14] its intensity after 25 min corresponds to 80% of that due to $Cu_A$.

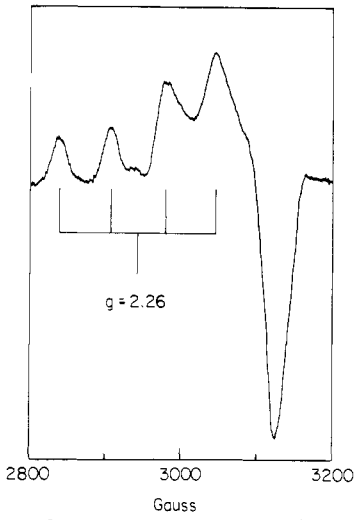


**Figure 3.** Unusual $Cu_B$ EPR spectrum observed after incubation of a cytochrome oxidase sample (initially fully reduced) for 45 s at 191 K. Conditions of EPR spectroscopy as in Figure 2. The observed hyperfine coupling is 137 G. Only the four features indicated are associated with the $Cu_B$ signal; the remaining features are due to $Cu_A$ and, to a lesser extent, $Fe_a$.

intensity of this signal reaches its maximum after approximately 5 min at 181 K; it then decays somewhat, leveling off after approximately 20 min. At times between 30 and 90 min, the signal intensity does not change appreciably; assuming $g_x$ and $g_y$ values of 1.3 (as suggested by the line-shape simulations described in ref 14), the $Cu_B$ signal intensity at this time corresponds to ca. 80% of that of $Cu_A$, consistent with Scheme I.

**Decay of the Unusual $Cu_B$ EPR Signal.** Subsequent steps in the dioxygen reduction reaction, which have not previously been investigated, were studied by raising the sample incubation temperature. The intensities of the $Cu_A$, $Fe_a$, and $Cu_B$ EPR signals after various times of incubation at 191.5 K are plotted in Figure 4. This sample was preincubated at a lower temperature (177 K) to produce the $Cu_A$, $Fe_a$, and $Cu_B$ EPR signals. At 191.5 K, the unusual $Cu_B$ signal decays to negligible intensity at a conveniently monitored rate (ca. $1.8 \times 10^{-3}$ $s^{-1}$). During the same period, the level of $Fe_a$ oxidation changes by less than 20% (in terms of the total number of oxidase molecules present) and that of $Cu_A$ by less than 10%. The changes in the $Fe_a$ and $Cu_A$ EPR signal intensities do not parallel the decay of the unusual $Cu_B$ EPR signal. After 1 h at 198 K, $Fe_a$ is still less than 50% as oxidized

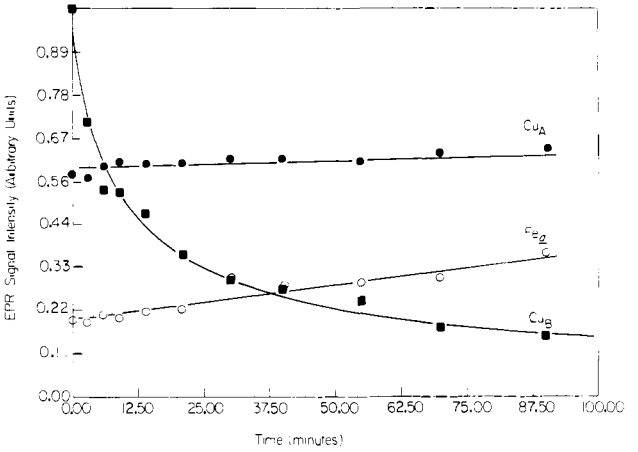


**Figure 4.** Intensities of the EPR signals due to $Cu_A$, $Fe_a$, and $Cu_B$ during incubation of a cytochrome *c* oxidase sample at 191.5 K. Initially reduced samples were preincubated at a lower temperature (177 K) for 2 h to produce the intermediate which exhibits the $Cu_B$ EPR signal. The lines through the $Cu_A$ and $Fe_a$ data points are drawn to guide the eye. The line through the $Cu_B$ data points is the best power law fit (eq 2). Conditions of EPR spectroscopy were as described in the legends to Figures 1 and 2.

**Table II.** First-Order Rate Constants[a] and Corresponding Temperatures for the Decay of the $Cu_B$ EPR Signal

| temp, K | $k_p$ $s^{-1}$ | temp, K | $k_p$ $s^{-1}$ |
|---|---|---|---|
| 207.0 | $(3.4 \pm 0.6) \times 10^{-2}$ | 193.0 | $(1.4 \pm 0.3) \times 10^{-3}$ |
| 203.0 | $(1.8 \pm 0.4) \times 10^{-2}$ | 191.5 | $(1.8 \pm 0.4) \times 10^{-3}$ |
| 203.0 | $(3.4 \pm 0.1) \times 10^{-2}$ | 187.0 | $(5.2 \pm 1.3) \times 10^{-4}$ |
| 202.5 | $(6.8 \pm 0.3) \times 10^{-3}$ | 183.0 | $(8.1 \pm 2.2) \times 10^{-5}$ |
| 197.0 | $(4.5 \pm 0.7) \times 10^{-3}$ | | |

[a] First-order rate constants were determined by a nonlinear least-squares fit to the power law expression given in eq 2. $k_p$ is the rate constant at the peak of the activation enthalpy distribution (see Experimental Section for details).

as is $Cu_A$, yet the unusual $Cu_B$ signal is almost completely gone. These observations imply that a process occurs at the $Fe_{a_3}/Cu_B$ site which is *independent* of the transfer of the fourth electron from either $Cu_A$ or $Fe_a$ and which causes the disappearance of the unusual $Cu_B$ signal. This would imply the existence of a second, EPR-silent intermediate at the three-electron level of dioxygen reduction.

The decay of the unusual $Cu_B$ signal is clearly nonexponential at all temperatures at which we have examined it. Nonexponential processes in proteins at low temperatures have previously been attributed to the existence of multiple conformations which have different activation enthalpies for the process and which do not interconvert.[22,23] The data for the decay of the unusual $Cu_B$ signal were well-fitted by the power law expression (ref 22, cf. Experimental Section) appropriate to such a situation. The line drawn through the $Cu_B$ points in Figure 4 is the best power law fit.

When the activation enthalpy takes on a range of values, its most probable value may be determined from the power law treatment if the process is examined over a range of temperatures.[22] Following incubation at 181 K for 90 min to produce the unusual $Cu_B$ signal, its decay was investigated at temperatures between 181 and 207 K. The decay curve at each temperature was fitted to the power law; the best fit kinetic parameters for the $Cu_B$ decay at various temperatures are compiled in Table II. The data in Table II were used to construct the Arrhenius plot in Figure 5. From the Arrhenius plot, we obtained a value of 18.1 ±1.6 kcal $mol^{-1}$ for the most probable activation enthalpy and a corresponding activation entropy of 21.4 ±8.2 cal $mol^{-1}$ $K^{-1}$, assuming a preexponential factor of $10^{13}$.[25]

**Further Oxidation of $Fe_a$.** As noted above, $Fe_a$ oxidation is not complete even after incubations which cause the nearly complete disappearance of the unusual $Cu_B$ signal. Continued incubation at 203 K causes further oxidation of $Fe_a$ to take place at a rate of approximately $8 \times 10^{-4}$ $s^{-1}$ (Figure 6). A comparison of the

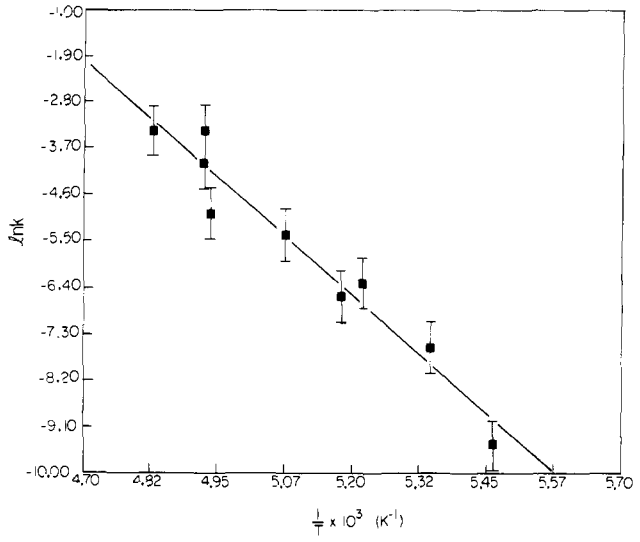


**Figure 5.** Arrhenius plot of the measured rate of decay of the unusual $Cu_B$ signal. The $Cu_B$ EPR signal intensities were fitted to a power law expression (see Experimental Section). The best linear least-squares fit to the data yields an activation enthalpy of 18.1 ± 1.6 kcal $mol^{-1}$ and an activation entropy of 21.4 ± 8.2 cal $mol^{-1}$ $K^{-1}$ (assuming a preexponential factor of $10^{13}$).

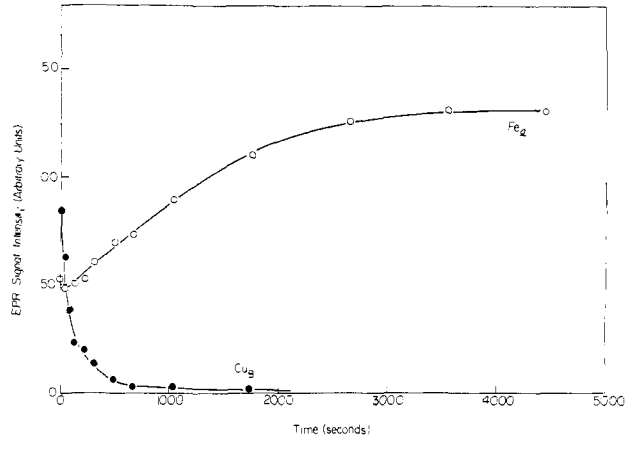


**Figure 6.** Intensity of the $Fe_a$ EPR signal during incubation of a cytochrome *c* oxidase sample at 203 K. Prior to the 203 K incubation, the sample was incubated at 177 K for 2 h. The behavior of the unusual $Cu_B$ signal during the 203 K incubation is also shown. The lines through the data points are drawn to guide the eye. Conditions of EPR spectroscopy were as described in the legends to Figures 1 and 2.

$Fe_a$ oxidation with the decay of the unusual $Cu_B$ signal again shows clearly that the two processes are not correlated: Most of the increase in the $Fe_a$ signal takes place *after* the unusual $Cu_B$ signal has decayed. Even after prolonged (more than 1 h) incubation at 203 K, $Fe_a$ oxidation is still not complete, however, as evidenced by a further increase in its intensity upon incubation at a somewhat higher temperature (211 K). Judging from the slowness of $Fe_a$ oxidation at 193 K (not shown) relative to that at 203 K, this process is rather highly activated. The activation enthalpy for this process was not determined, owing to the occurrence of other, complicating processes to be described below.

**Appearance of New Signals from Magnetically Isolated $Cu_B$ and $Fe_{a_3}$.** In an attempt to induce the complete oxidation of $Fe_a$ and measure its rate at a higher temperature, several samples with different histories were incubated at 211 K or higher. EPR spectra of a typical sample after incubation at 183 K, 211 K, and higher temperatures are shown in Figure 7. A new signal with splittings characteristic of a cupric ion appears upon incubation at 211 K. The *g* values and hyperfine coupling of this signal are the same as those of a signal assignable to $Cu_B$ which has previously been observed by Karlsson and Andréasson[17] by using a different method of sample preparation. During later stages of incubation at 211 K, and more so upon incubation at higher temperatures,

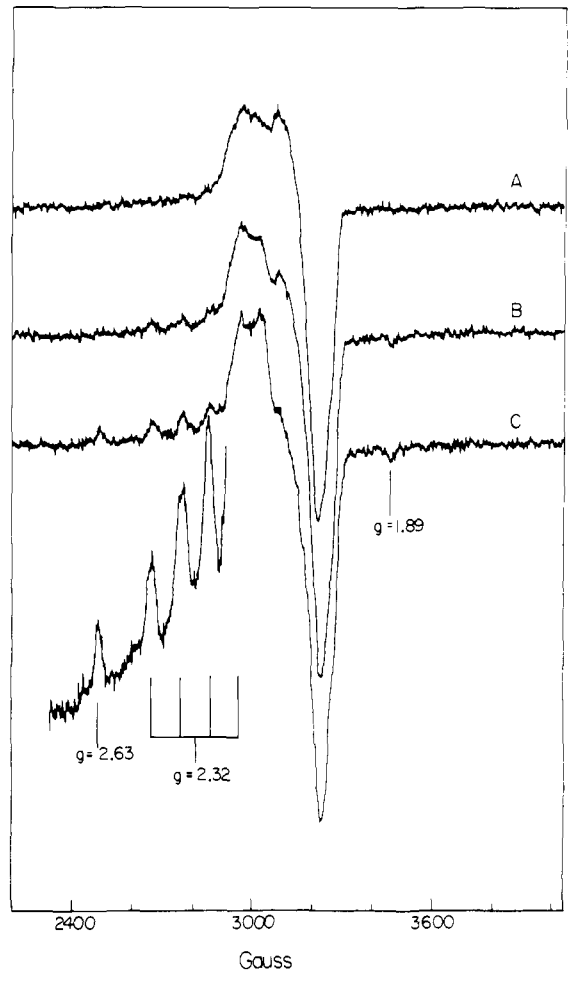


**Figure 7.** Development of new, magnetically isolated copper and iron EPR signals upon incubation at 211 K and higher temperatures. A: Spectrum of an initially reduced cytochrome *c* oxidase sample after incubation at 183 K for ca. 11 h. B: Spectrum after incubation at 211 K for 20 min. C: Spectrum after incubation at 211 K for 60 min, 216 K for 20 min, 223 K for 65 min, and 228 K for 16 min. For spectra A, B, and C, conditions of EPR spectroscopy were as described in the legend to Figure 1. The expansion of the low-field region is for the same sample as C but with microwave power of 0.20 mW and 4-fold higher gain.

another signal appears with features at $g = 2.63$ and $g = 1.89$, which is most plausibly assigned to low-spin $Fe_{a_3}$ coordinated by imidazole and hydroxide.[27,28] These signals exhibit no resolved dipolar splittings and are readily saturated, which indicates that they are due to magnetically isolated species, and they are not photolabile at 10 K. Concomitant with the appearance of these signals, $Fe_a$ undergoes some oxidation but again not to completion (as judged by the effect of thawing the samples, which causes a further increase in the $Fe_a$ signal intensity).

**Low-Temperature Oxidation of ca. Three-Fourths Reduced Cytochrome *c* Oxidase.** The role played by the fourth electron in the reaction of cytochrome oxidase with dioxygen may be investigated in low-temperature kinetic experiments using enzyme samples which are reduced by fewer than four electrons. The results of such an experiment are displayed in Figure 8, where we plot the intensities of the $Cu_A$, $Fe_a$, and unusual $Cu_B$ EPR signals during incubation at 181 K of a sample initially reduced by only 3.4 electrons. In this situation, most of the enzyme molecules contain only 3 reducing equiv at the beginning of the reaction. The important observations are, first, $Fe_a$ oxidation during this initial reaction step takes place to a much greater extent

(27) Lanne, B.; Malmström, B. G.; Vänngård, T. *Biochim. Biophys. Acta* **1979**, *545*, 205–214.
(28) Tang, S. C.; Koch, S.; Papaefthymiou, G. C.; Foner, S.; Frankel, R. B.; Ibers, J. A.; Holm, R. H. *J. Am. Chem. Soc.* **1976**, *98*, 2414–2434.

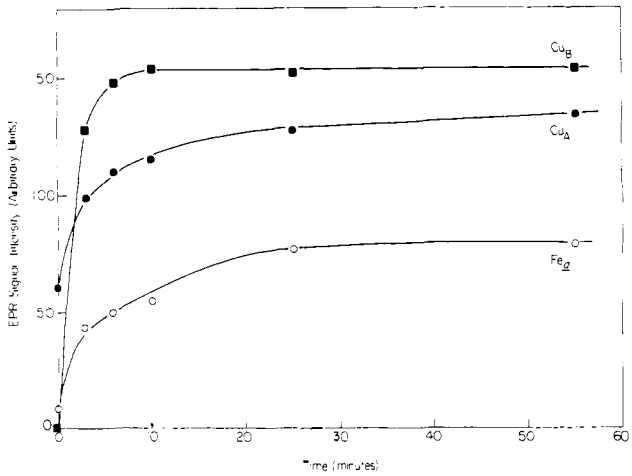


**Figure 8.** Intensities of the $Cu_A$, $Fe_a$, and unusual $Cu_B$ EPR signals during incubation of a partially (ca. 3.4 equiv) reduced cytochrome *c* oxidase sample at 181 K. The lines through the data points are drawn to guide the eye. Conditions were as noted in the legends to Figures 1 and 2. This figure should be compared with Figures 1 and 2, which depict an experiment which is identical except that it employs fully reduced enzyme.

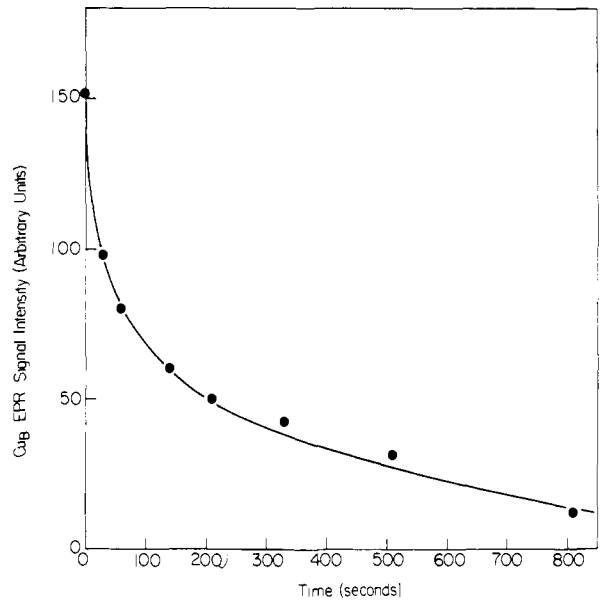


**Figure 9.** Decay of the unusual $Cu_B$ EPR signal during 205 K incubation of a cytochrome *c* oxidase sample initially reduced by 3.4 electrons. The sample was preincubated at 181 K for 55 min. to generate the unusual $Cu_B$ signal. Conditions of EPR spectroscopy were as described in the legends to Figures 1 and 2.

and at a slower apparent rate as compared to the situation in the fully reduced enzyme (compare with Figure 1) and, second, the unusual $Cu_B$ signal shows no early decay phase (compare with Figure 2).

The next step of the reaction, namely the decay of the unusual $Cu_B$ signal, was investigated by incubating the sample at 205 K. The unusual $Cu_B$ signal decays to near completion at a rate which is in agreement with rates measured with the fully reduced enzyme (Figure 9). This observation confirms that the transfer of the fourth electron to the dioxygen reduction site is not required for the elimination of the unusual $Cu_B$ signal, since most of the oxidase molecules do not contain a fourth electron.

The role of the fourth electron in producing the magnetically isolated $Cu_B$ and $Fe_{a_3}$ EPR signals was examined by incubating a three-electron-reduced sample at 203 K for 6 min followed by repeated incubations at 211 K or higher. The new copper and iron signals are produced in somewhat higher yield relative to the $Cu_A$ signal than in four-electron-reduced samples, particularly after 222 K incubation (spectra not shown). Some low-temperature kinetics samples were thawed for ca. 1 min at ice temperature to measure the changes in the $Cu_A$ and $Fe_a$ EPR signals. After the samples were thawed and refrozen, the magnetically isolated $Cu_B$ EPR signal appeared in considerably greater yield in a 3.4-electron-reduced sample than in a fully reduced sample.

**Solvent Dependence.** The solvent dependence of the low-temperature dioxygen reduction reaction was examined by conducting some experiments in 50% glycerol rather than in 40% ethylene glycol. The results of these experiments may be summarized as follows: The first reaction step, which involves the oxidation of $Fe_a$ or $Cu_A$ to produce the intermediate which exhibits the unusual copper EPR signal, was not substantially affected by the change in solvent. The unusual copper EPR signal was identical in appearance and was produced in similar yield. By contrast, the next reaction step, which involves the decay of the unusual copper signal, was significantly affected: In 50% glycerol, this process was approximately 100 times slower than in 40% ethylene glycol, requiring incubation temperatures some 15° higher to achieve comparable rates.

## Discussion

**Initial Reaction Steps.** The overall reaction scheme which best accounts for the initial electron-transfer events is shown above in Scheme I and is essentially identical with that deduced by Clore et al.[8] This scheme involves first the transfer of an electron from *either* $Cu_A$ or $Fe_a$, with similar apparent rates, to produce an intermediate at the $Fe_{a_3}/Cu_B$ site which is formally at the three-electron level of dioxygen reduction. This three-electron intermediate gives rise to the unusual $Cu_B$ EPR signal which exhibits only the features associated with one *g* value and which is unusually resistant to power saturation. At 181 K, both of these electron-transfer processes have an apparent first-order rate constant of ca. $4.4 \times 10^{-3}$ $s^{-1}$. Approximately 30% of $Fe_a$ and 70% of $Cu_A$ are oxidized in this step. The reduced $Cu_A$ which remains is oxidized in a somewhat slower process ($k$ = ca. $1 \times 10^{-3}$ $s^{-1}$). At 181 K, $Fe_a$ is still about 70% reduced after 2 h. Thus, after 2 h at 181 K, 70% of the $Fe_{a_3}/Cu_B$ sites are at the three-electron level of dioxygen reduction and exhibit the unusual $Cu_B$ EPR signal, while the remaining 30% are at the four-electron (formally, water) level.

The evidence for this reaction scheme consists of the following observations: (1) The careful kinetic analysis of Clore et al. showed convincingly that $Fe_a$ is oxidized in a single first-order step during incubation at a comparable temperature (173 K) and that $Cu_A$ oxidation is well-fitted by the expression appropriate to the two-step mechanism in Scheme I. All our data on the oxidations of $Fe_a$ and $Cu_A$ are consistent with this scheme: In numerous experiments at 181 K, the overall time course of $Cu_A$ oxidation was not well-fitted by a single exponential, and the oxidation of $Fe_a$ did not parallel that of $Cu_A$. After 2 h of incubation at 181 K, integration of the $Cu_A$ and $Fe_a$ signals shows that the amount of oxidized $Fe_a$ corresponds to much less than (approximately 30% of) the amount of oxidized $Cu_A$. (2) After subsequent incubation for 30 min at 203 K, the $Fe_a$ signal increases to approximately 80% of $Cu_A$. This indicates that a substantial percentage of the $Fe_{a_3}/Cu_B$ sites was in fact still at the three-electron level of dioxygen reduction after the incubation at 181 K, as required by Scheme I. At the same time, the $Cu_A$ signal does not increase appreciably, indicating that the oxidation of this site was very nearly complete at the lower temperature. (3) The $Cu_B$ signal, which is associated with an intermediate of dioxygen reduction at the three-electron level, shows a small but reproducible *decrease* at times between 5 and 10 min of incubation at 181 K. In the present reaction scheme, this decrease is caused by the elimination of some three-electron intermediate by the transfer of the fourth electron from $Cu_A$ to the $Fe_{a_3}/Cu_B$ site (the conversion from intermediate IIA to intermediate III). In samples initially reduced by only 3.4 electrons, in which the transfer of the fourth electron may not take place in most of the enzyme molecules, this early phase of $Cu_B$ decay was not observed.

The causes underlying the branched reaction scheme are in part revealed by the experiments using partially (ca. 3.5 equiv) reduced

enzyme samples. In the ca. 3.5-equiv reduced samples, $Fe_a$ is approximately 10% oxidized and $Cu_A$ is approximately 50% oxidized at the beginning of the experiment. In these samples, $Fe_a$ is oxidized to a much greater extent, approaching 80%, in the first electron-transfer step. This step is analogous to the conversion from intermediate I to intermediate IIA in Scheme I, differing only in that $Cu_A$ is already largely oxidized. In the partially reduced samples, the $Fe_a$ oxidation exhibits an apparent first-order rate constant which is approximately 2-fold smaller than that observed in the fully reduced samples. These observations are readily interpreted in terms of Scheme I. In the initial electron-transfer step of this scheme, the apparent rate constants for $Fe_a$ or $Cu_A$ oxidation in the case of the fully reduced enzyme will be the *sum* of the rate constants for the oxidations of these sites,[29] whereas in the case of the three-electron-reduced enzyme the apparent rate constants will be the same as the actual rate constants. The more extensive oxidation of $Fe_a$ in the ca. three-electron-reduced enzyme indicates that the electron transfer from $Fe_a$ is relatively fast if the electron is the third electron to be transferred to dioxygen but slow if it is the fourth. In the fully reduced enzyme, $Fe_a$ must compete with $Cu_A$ to be the donor of this third electron. It was previously suggested[8] that the trapping of the fourth electron in $Fe_a$ is due to an $Fe_a$–$Cu_A$ interaction, in which the oxidation of $Cu_A$ blocks the $Fe_a$ to $Cu_B/Fe_{a_3}$ electron transfer. The experiment using three-electron reduction shows that the contrary is the case: The presence of initially oxidized $Cu_A$ *increases* the amount of $Fe_a$ oxidation.

The first electron transfer from $Cu_A$ was examined over a range of temperatures between 166 and 186 K. The rate was estimated by using the slope of the early portion of the $Cu_A$ oxidation data, since at later times the curve is complicated by the second electron-transfer step (the conversion from intermediate IIA to intermediate III), in which some 30% of the $Cu_A$ oxidizes more slowly to yield the four-electron product at the $Fe_{a_3}/Cu_B$ site. The activation parameters deduced for the first electron transfer from $Cu_A$ are $\Delta H^{\ddagger} = 13.2 \pm 1.4$ kcal mol$^{-1}$ and $\Delta S^{\ddagger} = 2.8 \pm 7.7$ cal mol$^{-1}$ K$^{-1}$ (in a 40% ethylene glycol glass). This electron-transfer step showed only a weak dependence upon the nature of the medium: in a 50% glycerol glass, the rate was not markedly different from that in 40% ethylene glycol.

**Nature of the First Reaction Step.** While the initial processes which we have monitored, namely the oxidations of $Fe_a$ or $Cu_A$, must involve electron transfer from $Fe_a$ or $Cu_A$ to the dioxygen reduction site, it does not necessarily follow that the rates which we observe reflect the intrinsic rates of these electron transfers. It is possible that an event at the dioxygen reduction site must take place before the electron-transfer step may occur. If the electron transfers are rapid relative to this event, then the observed rate will be that of the process occurring at the dioxygen reduction site. In a recent low-temperature infrared absorption study, Fiamingo et al.[26] have shown that CO is not completely dissociated from the dioxygen reduction site by low-temperature photolysis. The CO molecules which are photolyzed from $Fe_{a_3}$ first bind to $Cu_B$ and then (in the absence of oxygen) recombine with $Fe_{a_3}$ in a second, slower step. Comparison with our measurements on the initial electron-transfer step reveals that at 181 K, the rate of CO recombination is comparable to that of $Cu_A$ oxidation, while the activation enthalpies for these processes are significantly different. The correspondence is close enough to suggest that the first process under examination in our experiments may in fact be the dissociation of CO from $Cu_B$, followed by relatively rapid reaction with iron-bound dioxygen to generate a peroxy intermediate and enable electron transfer from $Cu_A$ or $Fe_a$ (Scheme II).

It should be noted that the infrared absorption study was carried out in mitochondria suspended in 100% glycerol, while our most extensive studies were done with detergent-solubilized enzyme in 40% ethylene glycol. The difference in activation enthalpies may be related to the different reaction media employed or to the fact

**Scheme II**

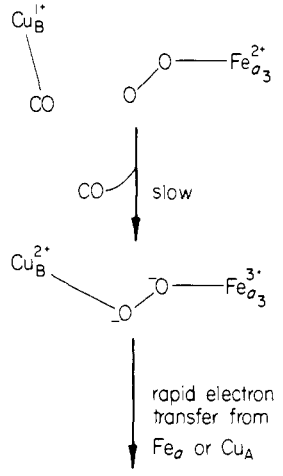


that the process monitored by Fiamingo et al., namely the simple reassociation of CO with $Fe_{a_3}$ in the absence of dioxygen, is different from that in the first step in Scheme II. Further studies of the medium dependence of this step and complementary studies of the dioxygen reaction by FT-IR will test the validity of Scheme II.

An examination of the first electron-transfer step in light of the long-distance electron-transfer theory lends some support to the idea that CO dissociation, and not electron transfer per se, is rate-limiting in the first oxidation step. An activation enthalpy as large as 13 kcal mol$^{-1}$ would imply that large structural rearrangements accompany the electron transfer. According to current electron-transfer theories,[30-32] the observed rate is surprisingly large given this large activation enthalpy and the intersite distances of ca. 15 Å which are implied by magnetic data.[33-35] However, if the rate-limiting factor is CO dissociation, then the actual activation enthalpy for the electron-transfer process may be much less than 13.2 kcal mol$^{-1}$, and electron-transfer rates which are well in excess of the observed overall rate (as required by Scheme II) would then be possible at intersite distances greater than 15 Å.

If Scheme II is correct, then the first intermediate in the low-temperature dioxygen reaction (probably a dioxygen adduct of ferrous $Fe_{a_3}$[8]) may differ from the physiologically relevant intermediate due to the involvement of the CO molecule bound to $Cu_B$. In the absence of CO, such an intermediate may never be formed or may have a very short lifetime. This possibility emphasizes the need to devise kinetic experiments, both at low and physiological temperatures, in which inhibitory ligands are not present.

**Second Reaction Step.** As noted above, an unusual EPR signal from $Cu_B$ appears in concert with the early oxidation of $Cu_A$ and $Fe_a$. Subsequent electron transfer from $Cu_A$ in the subpopulation of molecules which underwent initial oxidation at $Fe_a$ causes a portion of this signal to disappear, but most of the unusual $Cu_B$ signal, which is assigned to intermediate IIB in Scheme I, remains after 1 h at 181 K. The next distinct reaction step which is observed, after prolonged incubation at 181 K or much shorter incubation at temperatures ca. 10 deg higher, is the disappearance of this unusual $Cu_B$ signal. During this process, very little further oxidation of $Cu_A$ or $Fe_a$ takes place, and the time courses of $Cu_A$ and $Fe_a$ oxidation do not parallel the disappearance of the unusual $Cu_B$ signal. In samples which are initially reduced by only ca.

(29) Espenson, J. H. In "Chemical Kinetics and Reaction Mechanisms"; McGraw-Hill: New York, 1981; p 55.

(30) Hopfield, J. J. *Proc. Natl. Acad. Sci. USA.* **1974**, *71*, 3640-3644.
(31) Marcus, R. A.; Sutin, N. *Biochim. Biophys. Acta*, in press.
(32) Hopfield, J. J. In "Electrical Phenomena at the Biological Membrane Level"; Roux, E., Ed.; Elsevier: New York, 1977; pp 471-492.
(33) Brudvig, G. W.; Blair, D. F.; Chan, S. I. *J. Biol. Chem.* **1984**, *259*, 11001-11009.
(34) Mascarenhas, R.; Wei, Y.-H.; Scholes, C. P.; King, T. E. *J. Biol. Chem.* **1983**, *258*, 5348-5351.
(35) Ohnishi, T.; LoBrutto, R.; Salerno, J. C.; Bruckner, R. C.; Frey, T. G. *J. Biol. Chem.* **1982**, *257*, 14821-14825.

3.4 electrons, the unusual $Cu_B$ signal disappears to near completion and at the same rate as observed in fully reduced samples, indicating that the transfer of a fourth electron is not required for elimination of the three-electron intermediate which gives rise to the unusual $Cu_B$ signal. These observations imply that there are *two* intermediates at the three-electron level of dioxygen reduction, the first EPR-detectable and the second EPR-undetectable under the conditions of our experiments.

The conversion from the first to the second three-electron intermediate was characterized in considerable detail. This process exhibits markedly nonexponential behavior, which we attribute to the existence of multiple conformations which have different activation enthalpies for this step and which interconvert only slowly at these low temperatures. Analogous behavior has been observed in the recombination of CO with myoglobin[22] or with cytochrome oxidase[26] following photolysis. The progress of these reactions was satisfactorily fit by the power law expression (Experimental Section) which is appropriate to a distribution of activation enthalpies. We have found that the power law also gives a good fit to the conversion between the two three-electron intermediates. The power law analysis was used in conjunction with examination of this process over a range of temperatures to estimate the most probable activation enthalpy. The value which we deduce is 18.1 kcal $mol^{-1}$. The corresponding activation entropy is 21.4 cal $mol^{-1}$ $K^{-1}$ (assuming a prefactor of $10^{13}$, which is probably an overestimate). These activation parameters thus indicate that this step is entropically promoted to a substantial degree: An activation entropy of 21 cal $mol^{-1}$ $K^{-1}$ corresponds to a rate enhancement of approximately $4 \times 10^4$.

This step was also examined by conducting some experiments in 50% glycerol rather than in 40% ethylene glycol. In the glycerol glass, this step was much (ca. 100-fold) slower, taking place at an appreciable rate only at temperatures some 15 deg higher than the reactions in ethylene glycol. This result may reflect a change in the conformation of the enzyme, or its conformational flexibility, in the glycerol glass. The intensity and position of the $Cu_B$ signal are the same in the glycerol and ethylene glycol glasses, which suggests that the structure of the dioxygen reduction site is *not* substantially different. If the rate difference is caused by a difference in conformational flexibility, this would suggest that a significant protein conformational change is involved in this step.

The two three-electron intermediates are at the same formal oxidation level, but they must be structurally different since one exhibits an unusual copper EPR signal while the other does not. Various structures which contain the correct number of electrons may be envisaged, depending upon the state of the dioxygen bond and the extent of protonation. The activation parameters for the conversion process and the sensitivity of the process to conformation (which is implied by its distributed activation enthalpy) suggest that this process corresponds to the breaking of the dioxygen bond. The first of the three-electron intermediates would then contain a peroxidic adduct of ferrous $Fe_{a_3}$, while the second would contain a ferryl ion. Adopting this hypothesis, shown in Scheme III, we may say that the breaking of the O–O bond is promoted largely by a positive entropy change. Such a favorable entropy of activation could be achieved through ordering of the reactant state, in which hydroperoxide is coordinated to both the copper and the iron. If the intermetal distance is appropriate, the metals may act as a "rack"[36] on which the hydroperoxide is stretched and thereby ordered. Conversely, the hydroperoxide binding is expected to constrain the intermetal distance, thus decreasing the motional freedom of the surrounding protein.

The description shown in Scheme II applies to intermediate IIB only, since intermediate IIA is eliminated by a different pathway which involves the transfer of a fourth electron to the dioxygen reduction site. Following this electron transfer, the oxygen–oxygen bond may be broken, via a mechanism which is different from that in Scheme III or it may remain intact until the temperature is raised further. Since intermediate III is EPR-silent, other approaches will be required to study this alternate pathway. We only note here that the highly activated character of the reaction step in Scheme III makes it very likely that this path, which proceeds via two three-electron intermediates, will be the dominant one at physiological temperature, since the postulated bond-breaking step is predicted to be very rapid ($10^6$–$10^8$ $s^{-1}$) at 37 °C (by extrapolation of the Arrhenius plot in Figure 5).

**Scheme III**

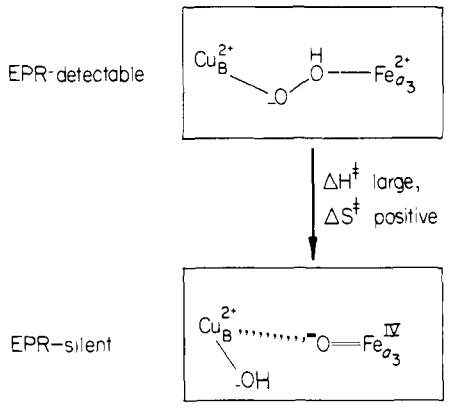


**Nature of the Unusual $Cu_B$ EPR Signal.** If Scheme III is correct, it must somehow account for the unusual EPR spectroscopic properties of the two three-electron intermediates. With regard to the first intermediate, we must explain why only a small portion of the copper EPR spectrum is observed and why this signal is very difficult to saturate relative to magnetically isolated copper species. Previously, in the absence of evidence for two different three-electron intermediates, this unusual $Cu_B$ EPR signal was proposed to arise from a cupric ion in proximity to a ferryl ion (the *second* three-electron intermediate in our reaction scheme). Additionally, it was proposed that a hydroxide ion coordinated to the copper is hydrogen-bonded to the ferryl oxygen, facilitating a superexchange interaction between the copper and iron spins.[14] The rapid relaxation of the copper spin and the absence of $g_x$ and $g_y$ features were ascribed to dipolar and/or superexchange coupling to the $S = 1$ (low-spin) ferryl ion, which is expected to relax fairly rapidly.[13,15,37]

In our reaction scheme, the unusual $Cu_B$ signal is proposed to arise from a hydroperoxide-bridged cupric/ferrous intermediate. In this intermediate, the hydroperoxide coordination to copper may be stronger than its coordination to iron; consequently, we propose that the ferrous iron is high-spin ($S = 2$) or intermediate-spin ($S = 1$). Neither of these spin states would be surprising given that the hydroperoxide coordination to copper could substantially weaken its coordination to iron. The peroxidic bridge between the copper and iron ions will facilitate a superexchange coupling between the ions. If the superexchange coupling parameter $J$ is small relative to the axial zero-field splitting $D$ of the high- or intermediate-spin heme, then perturbation theory may be used to calculate the $g$ values of the coupled cupric/ferrous spin system. This perturbation treatment shows that the superexchange coupling affects $g_x$ and $g_y$ to first order in $J/D$ but $g_z$ only to second order. The shape and intensity of the resolvable portion of the spectrum at $g_z$ is consistent with values for $g_x$ and $g_y$ less than or equal to 1.3.[13] Assuming an axial zero-field splitting of 20 $cm^{-1}$ and iron $g$ values of 2.0, the superexchange coupling required to give $g_x$ and $g_y$ values of 1.3 is calculated to be 3.5 $cm^{-1}$ if the iron is intermediate spin, or 1.1 $cm^{-1}$ if the iron is high spin. Using these value for $J$, the value of $g_z$ (which is perturbed only to second order in $J/D$) is predicted to be typical for copper, even if the $g$ values of the iron are quite anisotropic (e.g., $g_z(Fe) = 3.0$), which is itself unlikely. Similarly, the copper hyperfine coupling parameter $A_z(eff)$ will not be significantly reduced relative to the isolated copper ion.

(36) Lumry, R.; Eyring, H. *J. Phys. Chem.* **1954**, *58*, 110–120.

(37) Schulz, C. E.; Rutter, R.; Sage, J. T.; Debrunner, P. G.; Hager, L. P. *Biochemistry* **1984**, *23*, 4743–4754.

The absence of observable inflections near $g = 1.3$ could be caused by inhomogeneous broadening of the resonance, either by $g$ anisotropy in the iron (which would cause $g_y$ to be $> 1.3$ and $g_x$ to be $< 1.3$) and/or "$J$-strain", a distribution in the value of the superexchange coupling parameter $J$ caused by conformational heterogeneity. The resistance of the unusual $Cu_B$ EPR signal to power saturation also follows as a consequence of weak superexchange coupling to the iron ion. The presence of nearby higher-lying states in the iron spin manifold, which are admixed with the copper spin states, will facilitate the relaxation of the copper spin via the Orbach mechanism.[38] The temperature dependence of the $Cu_B$ relaxation rate is consistent with relaxation via an Orbach mechanism which involves spin excited states ca. 20 $cm^{-1}$ higher in energy.[39] Thus, all the properties of the unusual $Cu_B$ signal are accounted for by adopting the structure proposed in Scheme III and postulating a fairly weak (1.1 or 3.5 $cm^{-1}$, depending on the iron spin-state) superexchange interaction between the copper and the iron.

With regard to the second intermediate at the three-electron level of dioxygen reduction, which we suggest is in the cupric/ferryl oxidation state, we must explain why no EPR spectrum assignable to this intermediate is observed. The perturbation treatment described above, as well as an analogous treatment in which a very strong superexchange interaction is assumed and the zero field splitting is treated as a perturbation, indicates that in the limits of very strong or very weak coupling, the superexchange interaction cannot make the expected resonance so anisotropic or so inhomogeneously broadened that all its spectral features, particularly those at $g_z$, are undetectable. However, at intermediate strengths of the superexchange coupling (which would require a higher-order calculation for quantitative characterization), it is possible that the $g_x$ and $g_y$ values could be lowered, shifting these resonances to much higher field, so that even the resonance at $g_z$ became undetectable. Using the formulas of Aasa and Vanngard,[21] we calculate that a shift in $g_{x,y}$ from 1.3 to ca. 0.5 would result in a 10-fold reduction in the area of the peak at $g_z$. In the $S(Fe) = 1$, $S(Cu) = {}^1/_2$ system, this would require a superexchange coupling of 8 $cm^{-1}$, using the above perturbation treatment. (However, since $J/D = 0.4$ in this case, this calculation must be considered approximate.) We note that if there is even a weak bond between the ferryl oxygen and the copper ion, the superexchange coupling between the metals could be much stronger in the ferryl-containing intermediate than in the hydroperoxide-bridged intermediate and quite possibly as strong as 8 $cm^{-1}$. Another possible explanation for the absence of an EPR signal from the second three-electron intermediate is that spin relaxation in this cupric/ferryl system is very rapid ($1/T_2 = 10^{10}$ $s^{-1}$), so that the spectral features are broadened beyond detection.

**Third Reaction Step.** In the third step of the reaction, an additional fraction of $Fe_a$ is oxidized. This takes place at conveniently monitored rates at temperatures near 203 K. At ca. 193 K, $Fe_a$ oxidation takes place much more slowly, so this step is rather highly activated. Precise measurement of the activation enthalpy was not made. As discussed above, the slowness of this oxidation is related to the fact that the electron in $Fe_a$ at this step is the *fourth* electron to take part in the dioxygen reaction; when it is the third electron, the transfer occurs more rapidly. This indicates that the different electron transfers which take place during the dioxygen reduction reaction can have significantly different rates, even when the electron donor is the same. This is not surprising in view of the changes which are necessarily taking place at the dioxygen reduction site during the reaction cycle.

**Fourth Reaction Step: Generation of a Magnetically Isolated $Cu_B$ EPR Signal.** In samples which had previously been incubated at 203 K or lower temperature, subsequent incubation at 211 K for 20–40 min caused the appearance of a new EPR signal with hyperfine splittings which indicate that it is due to copper. The saturation behavior of this signal was not unusual for copper; i.e., it was significantly saturated by submilliwatt microwave powers

**Scheme IV**

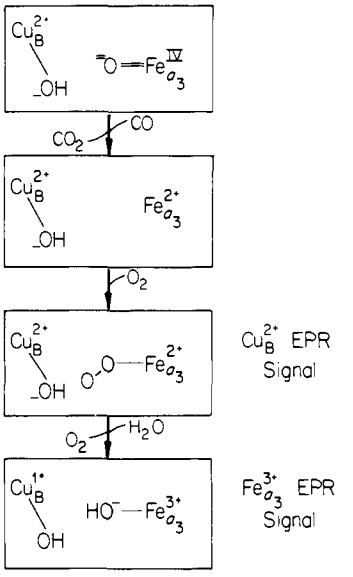


at 9 K, and it exhibits no dipolar splittings to suggest that it is in proximity to another paramagnet. This signal has been described previously under different conditions of sample preparation[17] and was assigned to $Cu_B$. Since complete recovery of the normal $Cu_A$ signal intensity is observed after incubation at the lower temperatures, we also conclude that the signal is due to $Cu_B$. The absence of splittings or unusual saturation behavior indicates that the nearby $Fe_{a_3}$ is diamagnetic, i.e., low spin ferrous. If incubation is continued at 211 K or higher, another signal appears at $g = 2.63$ and 1.89, which may be assigned to low-spin ferric $Fe_{a_3}$.[27,28] This signal, like the magnetically isolated $Cu_B$ signal, exhibits no splittings to suggest the proximity of another paramagnet, indicating that the nearby $Cu_B$ is reduced. Both of the EPR signals from the dioxygen reduction site which appear upon incubation at 211 K thus arise from states in which the site contains a single reducing equivalent.

Because we have proposed that the dioxygen reduction site is already in a highly oxidized (ferryl–cupric) state after the low-temperature incubations, its partial reduction at 211 K is at first somewhat puzzling. A source for the electrons, apart from $Fe_a$ and $Cu_A$, is required to explain this reduction. A variety of evidence suggests that this electron source is carbon monoxide, which reduces the site via the reaction in Scheme IV.

After the lower temperature incubations, and after the 211 K incubations which led to the generation of the new signals, $Fe_a$ oxidation was still not complete. These observations are as required by Scheme IV. In a sample initially reduced by only ca. 3.4 electrons, incubation at 211 K led to the generation of the magnetically isolated $Cu_B$ and $Fe_{a_3}$ signals in higher yield. Upon thawing samples which had been used in kinetic studies at ca. 200 K or lower for 1 min at ice temperature, little of the magnetically isolated $Cu_B$ signal was seen if the samples had been initially reduced almost completely, but a substantial quantity was produced in samples which had been initially reduced by only 3.4 equiv. These results suggest that a three-electron intermediate is involved in the production of the magnetically isolated $Cu_B$ EPR signal.

Alternate explanations for the appearance of the magnetically isolated EPR signals which do not involve the rereduction of this site must postulate that the iron–copper pair was not oxidized to the ferryl–cupric level at the lower incubation temperatures. Such explanations would require that there be *three* intermediates at the three-electron level of dioxygen reduction and that the dioxygen bond be intact in all three of them. The different EPR properties of the three intermediates would then be due to changes in the iron–copper coupling and the iron spin state. This kind of explanation appears unlikely to be true, especially in view of the stability of the new $Cu_B$ signal for at least 1 min at 273 K.

(38) Orbach, R. *Proc. R. Soc. London, Ser. A* **1961**, *264*, 458–484.
(39) Malmström, B. G., unpublished results.

The oxidation of carbon monoxide which is proposed in Scheme IV is noteworthy because it takes place at an appreciable rate ($t_{1/2}$ ca. 20 min) at relatively low temperature (211 K) and significantly faster ($t_{1/2}$ less than 1 min) at ice temperature. This is perhaps surprising in view of published reports on the reduction of cytochrome oxidase[40] or hemin[41] by carbon monoxide. However, the latter reactions take place in ferric–cupric or ferric systems, in contrast to the reaction in Scheme IV, which involves a ferryl ion. The ferryl ion, with the structure proposed, is well-suited to this reaction in two respects: It is able to accept two electrons at once, and it contains an oxygen atom which is not protonated.

**Electron-Transfer Pathways.** We conclude by noting one of the implications of the scheme describing the early electron-transfer events. This scheme involves the partitioning of the oxidase molecules into two distinct populations by transfer of the first electron from either $Fe_a$ or $Cu_A$. The occurrence of this partitioning indicates that both $Cu_A$-to-$Fe_{a_3}/Cu_B$ site and $Fe_a$-to-$Fe_{a_3}/Cu_B$ site electron-transfer pathways are approximately equally competent at these temperatures. The similarity of the rates via the two paths indicates that one is not very much better than the other with respect to the distance of the transfer or the suitability of the intervening material.[30] The existence of two competent electron pathways to the dioxygen-reduction site may have implications for the mechanisms of energy conservation by the oxidase. It is now well-established that the cytochrome oxidase-catalyzed transfer of electrons from cytochrome *c* to dioxygen is coupled to the active transport of protons across the mitochondrial membrane,[4] and it appears most likely that either $Fe_a$ or $Cu_A$ is involved in this proton pumping function. If, for example, $Cu_A$ were the proton pump, then the $Fe_a$-to-$Fe_{a_3}/Cu_B$ electron-transfer path would bypass the pump. Such a bypass mechanism might be important at steps in dioxygen reduction where the $Cu_A$-to-$Fe_{a_3}/Cu_B$ transfer, which is linked to proton pumping, is relatively slow because these steps are not sufficiently exothermic. It has been suggested[42] that proton pumping might be uncoupled from electron transfer at some steps in the cytochrome oxidase reaction cycle. The existence of two competent electron-transfer pathways to the dioxygen-reduction site may reflect the need for this uncoupling.

**Acknowledgment.** Supported by Grant GM-22432 from the National Institute of General Medical Sciences, U.S. Public Health Service, and by BRSG Grant RR07003 awarded by the Biomedical Research Support Grant Program, Division of Research Resources, National Institutes of Health. D.F.B. was recipient of National Research Service Award 5T32GM-07616 from the National Institute of General Medical Sciences.

**Registry No.** $O_2$, 7782-44-7; CO, 630-08-0; $CO_2$, 124-38-9; cytochrome *c* oxidase, 9001-16-5; glycerol, 56-81-5; ethylene glycol, 107-21-1.

(40) Nicholls, P.; Chanady, G. A. *Biochim. Biophys. Acta* **1981**, *634*, 256–265.
(41) Bickar, D.; Bonaventura, C.; Bonaventura, J. *J. Biol. Chem.* **1984**, *259*, 10777–10783.
(42) Blair, D. F.; Gelles, J.; Chan, S. I. *Biophys. J.*, submitted for publication.

# Reactions of $CoCp^+$ (Cp = Cyclopentadienyl) with Hydrocarbons in the Gas Phase. Observation of Novel Skeletal Isomerizations/Dehydrocyclizations Resulting in Cobaltocenium Formation

**D. B. Jacobson† and B. S. Freiser***

*Contribution from the Department of Chemistry, Purdue University, West Lafayette, Indiana 47907.* *Received March 26, 1985*

**Abstract:** The gas-phase reactions of $CoCp^+$ with a variety of hydrocarbons are described by using Fourier transform mass spectrometry (FTMS). All aliphatic alkanes larger than methane (except 2,2-dimethylpropane) are dehydrogenated by $CoCp^+$ with no C–C bond cleavages observed. Collisional activation of $CoCp(olefin)^+$ species derived from $C_5$ and $C_6$ alkanes, as well as reactions of $CoCp^+$ with isomeric pentenes and hexenes, are dominated by skeletal isomerization followed by dehydrocyclization forming cobaltocenium. Dehydrocyclization of linear $C_5$ olefins is more facile than skeletal isomerization of branched $C_5$ olefins. Reactions with cyclopropane and cyclobutane proceed by initial insertion across the strain-weakened C–C bonds. For cyclopropane, insertion into a C–C bond results in initial formation of a cobaltacyclobutane species which undergoes dehydrogenation exclusively. With cyclobutane, both dehydrogenation and symmetric ring cleavage occur for the cobaltacyclopentane species. $CoCp^+$ reacts with cyclopentane and cyclohexane by attacking C–H bonds exclusively. Finally, $D°(CoCp^+–Cp) = 118 \pm 10$ kcal/mol and $D°(Co^+–Cp) = 85 \pm 10$ kcal/mol are assigned from the observed reactivities.

Atomic transition-metal ions have proven to be highly reactive in the gas phase. This has been demonstrated by several recent investigations on the reactions of gas-phase transition-metal ions with a variety of organic species using ion cyclotron resonance (ICR)[1–4] spectrometry, Fourier transform mass spectrometry (FTMS),[5,6] and ion beam techniques.[7,8] The first-row groups 8–10 transition-metal ions have received the most attention which has resulted in a good understanding of their reactions with a variety of simple hydrocarbons. In general, these atomic metal ions react with aliphatic alkanes by attacking C–C bonds predominantly.[2,4d,6a,7a,b,8]

The reactivity of organometallic fragment ions with hydrocarbons is particularly interesting since the intrinsic effect that

†Current Address: 127-72 Noyes Laboratory, Department of Chemistry, California Institute of Technology, Pasadena, California 91125.

(1) (a) Allison, J.; Ridge, D. P. *J. Organomet. Chem.* **1975**, *99*, C11. (b) Allison, J.; Ridge, D. P. *J. Am. Chem. Soc.* **1976**, *98*, 5700. (c) Allison, J.; Ridge, D. P. *J. Am. Chem. Soc.* **1976**, *98*, 7445. (d) Allison, J.; Ridge, D. P. *J. Am. Chem. Soc.* **1977**, *99*, 35. (e) Allison, J.; Ridge, D. P. *J. Am. Chem. Soc.* **1978**, *100*, 163. (f) Allison, J.; Ridge, D. P. *J. Am. Chem. Soc.* **1979**, *101*, 4498.
(2) (a) Allison, J.; Freas, R. B.; Ridge, D. P. *J. Am. Chem. Soc.* **1979**, *101*, 1332. (b) Freas, R. B.; Ridge, D. P. *J. Am. Chem. Soc.* **1980**, *102*, 7129. (c) Larsen, B. S.; Ridge, D. P. *J. Am. Chem. Soc.* **1984**, *106*, 1912.
(3) (a) Lombarski, M.; Allison, J. *Int. J. Mass. Spectrom. Ion Phys.* **1983**, *49*, 281. (b) Huang, S. K.; Allison, J. *Organometallics* **1983**, *2*, 883. (c) Tsarbopoulos, A.; Allison, J. *Organometallics* **1984**, *3*, 86. (d) Radecki, B. D.; Allison, J. *J. Am. Chem. Soc.* **1984**, *106*, 946.

0002-7863/85/1507-7399$01.50/0 